JMEPEG (2012) 21:69–73
DOI: 10.1007/s11665-010-9818-7

1059-9495/$19.00

Yield Stress of 21-6-9 Stainless Steel Over Very Wide Ranges of Strain Rates and Temperatures

M.E. Kassner and P. Geantil

(Submitted May 28, 2010; in revised form November 11, 2010)

The yield strength of solution-annealed 21-6-9 austenitic stainless steel was determined over a wider temperature range (−195 to 1100 °C) and strain rate (10^{-4} to 10^{4} s^{-1}) than has been previously reported. The most noteworthy characteristic of the variation of yield stress with temperature was the dramatic decrease in yield strength from −195 to 300 °C. The strain-rate sensitivity exponent, *m*, was determined using strain-rate change tests. *m* dramatically increases at about 850 °C with increasing temperature and *m* is approximately independent of strain (structure). Hopkinson split-bar tests from ambient temperature to 750 °C indicate that the strain-rate sensitivity of 21-6-9 is not strongly influenced by the over eight orders of magnitude change in strain rate. This suggests that the mechanism(s) of plastic flow at the higher rates is similar to that at lower rates. This contention was corroborated by transmission electron microscopy. The yield stress shows grain-size dependency.

Keywords mechanical testing, metallography, stainless steels

1. Introduction

21-6-9 stainless steel is of great interest due to its excellent toughness, particularly at cryogenic temperatures, its ductility, and like other austenitic steels, its nonmagnetic quality. The excellent material properties make these steels useful in applications ranging from fusion reactors to the aerospace industry (Ref 1-3). Efforts to do finite element analysis of structures made from this steel require that a number of material properties be known, yield strength, and strain-rate sensitivity being important ones (Ref 4).

This article reports the effects of strain rate (10^{-4} to 10^{4} s^{-1}) and temperature (−196 to 1100 °C) on the yield strength of 21-6-9 austenitic stainless steel. The strain-rate sensitivity exponent, *m*, was determined and is defined as

$$m = \left(\frac{\partial \ln \sigma}{\partial \ln \dot{\varepsilon}}\right)_{\varepsilon,T} \quad \text{(Eq 1)}$$

where σ is stress, $\dot{\varepsilon}$ is strain rate, T is temperature, and ε is strain. The values of *m* were determined over the same temperature range of −196 to 1100 °C. The effect of grain size on the yield stress was also assessed.

Transmission electron microscopy was performed on compression specimens deformed at strain rates of approximately 10^{-4} s^{-1} and 600 s^{-1}. The character and arrangement of defects on specimens deformed at the high and low strain rates were compared. These comparisons provide insight into the plastic flow over eight orders of magnitude in strain rate.

M.E. Kassner and **P. Geantil**, Departments of Aerospace and Mechanical Engineering, Materials Science, University of Southern California, Los Angeles, CA 90089-1455. Contact e-mail: petertrain@gmail.com.

2. Experimental Procedure

The 21-6-9 austenitic stainless steel used in this study was provided in the form of 76 mm diameter stock. The chemical analysis is given in Table 1. Tensile specimens were machined from this stock to a 6.4 mm diameter round with a 51 mm gauge length. All specimens were initially solution annealed at 1080 °C for 1 h in vacuum. The resulting average grain intercept was about 26 μm. The annealing temperature and duration were identical to those used in a similar study (Ref 4).

In this study, the strain-rate sensitivity exponent, *m*, was determined by strain-rate change tests. This kind of test is illustrated in Fig. 1. In this test, the stainless steel is deformed from the solution-annealed condition at the strain rate of 10^{-4} s^{-1}. After a specific amount of plastic strain (0.002, 0.03, or 0.15 in this study), the imposed strain rate is changed to the higher rate of 10^{-2} s^{-1}. In response to this change, the stress elastically "jumps" from the value of σ_1 (Fig. 1). Eventually, the material plastically deforms at this higher strain rate. With the experimental apparatus used, the onset of plastic deformation can only be discriminated after about 0.0002 plastic strain (σ_2, Fig. 1). Since 0.0002 plastic strain is small, the structures at σ_1 and σ_2 can be regarded as identical. Therefore, the stress exponent *m*, can be approximated by

$$m = \left(\frac{\partial \ln \sigma}{\partial \ln \dot{\varepsilon}}\right)_{\varepsilon,T} = \frac{\ln(\sigma_2/\sigma_1)}{\ln(\dot{\varepsilon}_2/\dot{\varepsilon}_1)} \quad \text{(Eq 2)}$$

where *m* is a constant-structure stress exponent.

Hopkinson split bar compression specimens were machined from the same stock; they were also of 6.4 mm diameter with either 6.3 or 12.6 mm length. All specimens were solution-annealed, again, at 1050 °C for 1 h in a vacuum. This is a slightly different temperature than the one used for the tensile

Table 1 Composition of 21-6-9 stainless steel

Element	Analysis, wt.%
Chromium	19.81
Nickel	7.23
Manganese	9.38
Carbon	0.02
Silicon	0.09
Phosphorus	0.011
Sulfur	0.01
Nitrogen	0.3
Iron	Balance

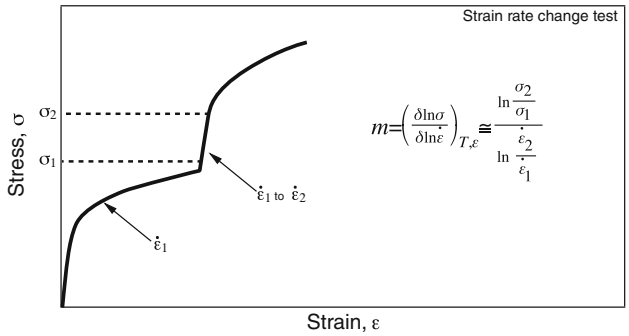

Fig. 1 Variation of yield stress of annealed 21-6-9 stainless steel with temperature

specimens; however, it has been used in similar studies, and both have shown to cause a modest amount of grain growth (Ref 4). Neither temperature is preferred in this case (Ref 5).

Mechanical testing at strain rates of 10^{-1} s^{-1} and below was performed in tension on an Instron 10,000-lb screw-drive model TTC-L. The yield stress was determined using a 0.2% plastic-strain offset. At strain rates within the range 10^{-1} s^{-1} to 10^{0} s^{-1}, yield stresses were determined from tensile tests using an MTS 10,000-lb test system with a transient-data-acquisition system. Again the yield stress was determined using a 0.2% plastic-strain offset.

The facility used for the Hopkinson split-bar testing is described in detail elsewhere (Ref 6). For these compression tests, the stress-vs.-strain behavior cannot be meaningfully described at plastic strains less than the range 2 to 5%. In these cases, the 0.2% plastic-strain offset was extrapolated. This was done assuming that the stress-vs.-strain behavior in the 2 to 5% range is about the same as that of specimens deformed at lower (10^{-4} s^{-1}) strain rates and at lower temperatures, so that the flow stresses were comparable to those encountered at split-bar strain rates. If, for high strain-rate tests, the stress-vs.-strain behavior could not be meaningfully described below 5% strain, then the stress-vs.-strain curve from 0 to 5% strain at 77 K and 10^{-4} s^{-1} was used to extrapolate the 0.2% strain flow stress from the 5% strain flow stress at the high strain rate. In all cases, the extrapolation was linear to within 5% of the flow stress. High-temperature split-bar tests were performed by heating the specimen in a furnace in which the test specimens were suspended by a copper wire in such a manner that they were in line with the testing bars. These bars were quickly inserted into the furnace so that they contacted the specimen. The test was then quickly commenced.

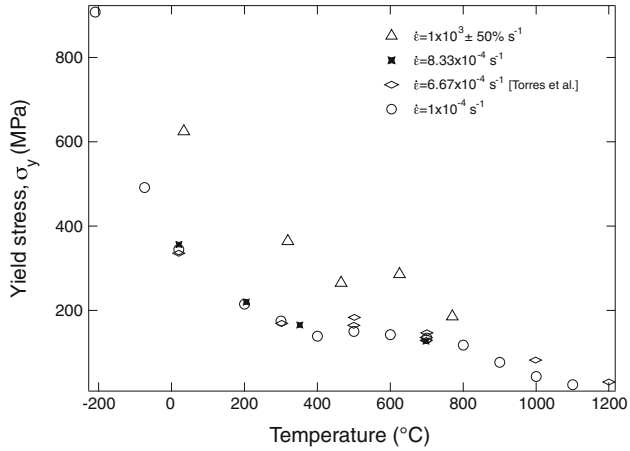

Fig. 2 The elevated-temperature yield stress of annealed 21-6-9 stainless steel as a function of temperature for a high and low strain rate

For the grain-size part of the study, tensile specimens were machined from this stock to a 6.4 mm diameter round, with a 51 mm gage length. All specimens were initially solution annealed at 1080 °C for 1 h in vacuum. Some specimens had an additional anneal of 1165 °C for 40 min in vacuum to increase the grain size to about 104 μm.

3. Results and Discussion

Figure 2 shows the variation of the yield stress of 21-6-9 stainless steel with temperature. The most impressive characteristic of the data is the dramatic decrease in yield strength from −196 to 300 °C. There is then a plateau from 300 to 600 °C, followed by a further decrease in yield strength. The plateau region is common in such studies, and is caused by solute atoms present in the alloy (Ref 7, 8). Three different yield strength tests were conducted and reported here, while one additional is reported from a similar study done by Torres et al. (Ref 4). All the data from our study along with Torres et al. agrees well. It is worth noting that the ultimate tensile stress study from Ref 4 shows a similar behavior, with a plateau from the same relative temperatures. This is caused by the solute atoms as well, particularly the interstitials carbon, nitrogen, and oxygen.

Equation 1 predicts that the yield strength changes with changes in the applied strain rate. The relative change depends on the size of the exponent, m. Large values of m suggest high strain-rate sensitivity (i.e., relatively large changes in yield stress for a given change in strain rate). Figure 3 plots values of m with changes in temperature. The m data are reported for strain-rate change tests performed after total plastic strains of 0.002 (essentially the annealed structure), 0.03, and 0.15. Two impressive features are observed from Fig. 3: first, m dramatically increases at about 850 °C, and second, m is approximately independent of strain (structure). At the higher temperatures (T = 800 °C), the steady-state or maximum flow stress is attained at strains less than 0.03. Therefore, strain-rate change tests appear unnecessary at higher strain levels. This change in m at higher temperatures has been observed in other materials as well, above about half the absolute melting temperature (0.5 T_m) (Ref 9).

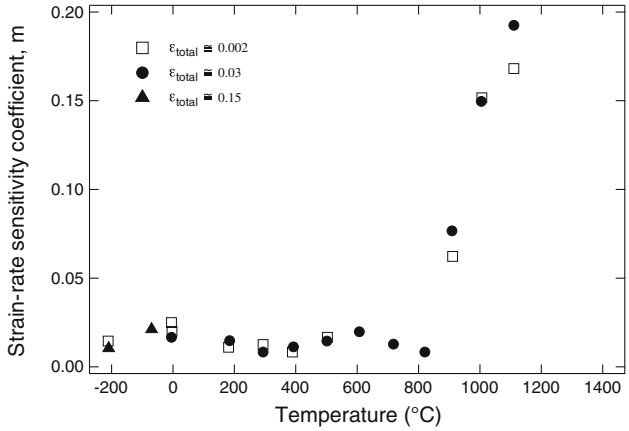

Fig. 3 Variation of constant-structure strain-rate sensitivity exponent, m with temperature and strain

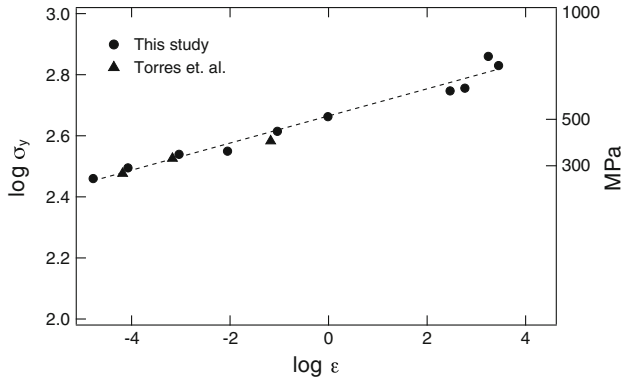

Fig. 4 The ambient-temperature yield stress of annealed 21-6-9 stainless steel as a function of strain rate

It should be mentioned that, at ambient temperature, m for annealed 21-6-9 has an average value of about 0.022. It is observed that this is a lower m than in Fig. 4, where the 0.2% plastic strain offset is plotted as a function of strain rate at ambient temperature. This disparity can be explained, in part, by the fact that in Fig. 4, m was determined by comparing the 0.2% offset yield stress of different annealed specimens, deformed at different strain rates. In this case,

$$m = \frac{\ln(\sigma_{y_2}/\sigma_{y_1})}{\ln(\dot{\varepsilon}_2/\dot{\varepsilon}_1)} \qquad \text{(Eq 3)}$$

That is, m was determined by measuring the slope of the indicated best-fit line in Fig. 4. The value of m determined from the six tensile tests at strain rates less than 1 s^{-1} was 0.038, somewhat larger than Fig. 3 data, however, additional data from Torres et al. (Ref 4) is plotted and agrees well, with their m value of 0.034. This small discrepancy is most likely due to the slight variation in alloy compositions used. Perhaps the m values determined from the yield-stress difference technique (Eq 3) with 0.002 offsets are higher than those determined using the strain rate change test (Eq 2) using 0.002 offsets because the assumption of constant structure is more relaxed in the former case. That is, a fraction of the difference between the yield stresses at the different strain rates for different specimens is partly accounted for by a difference in substructure. Additional uncertainty is introduced using different specimens in Eq 3.

The best-fit line in Fig. 4 includes the Hopkinson split-bar rates (10^2 to 10^4 s^{-1}). Note that the data from the four Hopkinson split-bar tests are in very close proximity to the line. This suggests that the value of the strain-rate sensitivity of 21-6-9 at "quasi-static" rates (10^{-4} to 10^{-1} s^{-1}) is also appropriate at much higher rates (1 to 10^4 s^{-1}), and that the controlling mechanism of plastic deformation (thermal activation of dislocations over short-range barriers) in 21-6-9 persists over a wide range (10^{-4} to 10^4 s^{-1}) of plastic flow-rates. Changes in the controlling mechanism of plastic deformation in metals seem to be associated with dramatic changes in m. Above about half the homologous melting temperature (low stress and strain rate), dislocation climb is generally accepted as the controlling mechanism for plastic deformation and m is about 8 (Ref 9). Below about half the homologous melting temperature, the controlling mechanism changes to thermally activated dislocation glide, and m increases to generally much higher values.

The suggestion that the rate-controlling mechanism for plastic flow is the same over the wide range of flow rates considered seems to also be reasonable over a wide range of temperatures. In Fig. 2, the yield stress of 21-6-9 is plotted as a function of temperature (−196 to 1100 °C) for a strain rate of 10^{-4} s^{-1}. Also illustrated are the data from the five sets of Hopkinson split-bar tests for which the strain rate was within the range of 10^3 s^{-1} (±50%). Note that the general stress-vs.-strain-rate behavior at the high strain rate is the same as at the low strain rate. This is consistent with the data of Fig. 3. At each temperature in Fig. 2, the magnitude of increase in yield stress associated with the increased strain rate is predictable in terms of the value of the strain-rate sensitivity of Fig. 3. We did not observe m to change dramatically over the present range of temperatures to 750 °C. Above about 850 °C m changes to much higher values.

The data of Fig. 3 and 4 are consistent with 304 stainless steel data in (Ref 10). These sorts of trends were also observed at higher temperatures in mild steel by Campbell and Ferguson (Ref 11) and in Nb and Mo by Briggs and Campbell (Ref 12), and at low temperatures in several alloy steels (Ref 13).

The contention that the nature of plastic flow at the high strain rates is the same as at the lower rates was also checked by transmission electron microscopy (TEM). The microstructures of two compression specimens deformed to a strain of 0.063 were examined, one at a strain rate of 10^{-4} s^{-1} and the other at 600 s^{-1}. In both the specimens, planar arrays of dislocations, stacking faults, and occasional mechanical micro-twins were observed. In all the observed grains, for both specimens, there were two active slip systems. Perhaps, a somewhat increased density of these features was observed in the Hopkinson split-bar ($\dot{\varepsilon} = 600\,s^{-1}$) specimen. A stereo pair (2½-D) of micrographs are illustrated in Fig. 5 for the high strain-rate specimen.

Regarding the composition of the alloy, it is well known that the nitrogen additions lower the stacking fault energy (SFE) particularly when increasing from 0.21 to 0.24 wt.%. This in turn promotes a transition to a more planar plastic deformation mode. The lower SFE additionally increases the tendency for deformation twins and stacking faults (Ref 14, 15). It is also well established that increased nitrogen content increases the yield strength and stabilizes the austenitic phase (Ref 16). Interestingly in other austenitic steels, nitrogen has not only shown a solute strengthening effect but also increases the grain size strengthening effects, and k_y increases linearly with the nitrogen content (Ref 17) although this effect was not studied

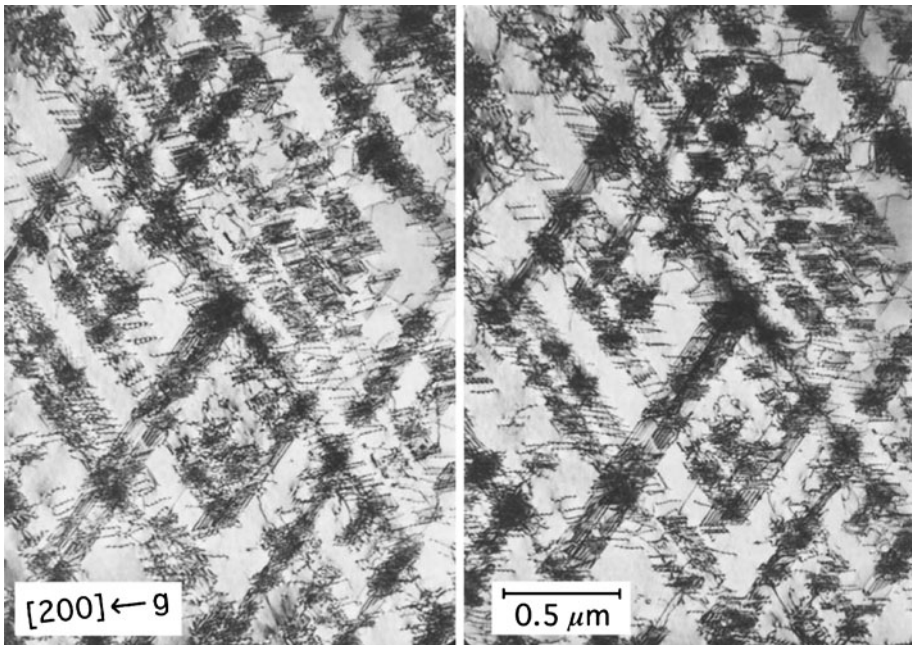

Fig. 5 Transmission electron micrograph of a 21-6-9 stainless steel specimen strained 6.3% at ambient temperature and a strain rate of 600 s^{-1}. z = [001] **g**⟨200⟩ stereo pair

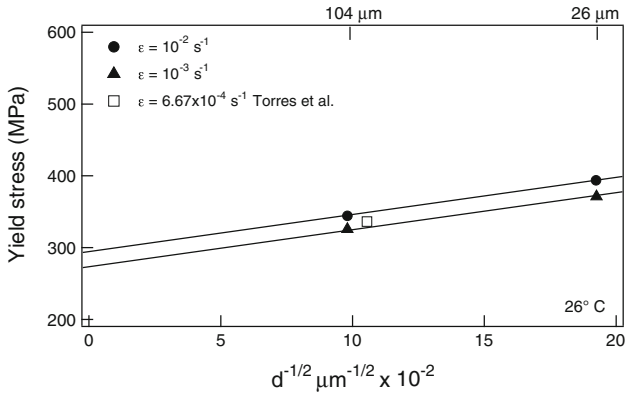

Fig. 6 The effect of grain size on the yield strength of annealed stainless steel for two different strain rates is illustrated

here. The effects of manganese on the SFE are somewhat debated and less clear than nitrogen, but it is known that it has little, if any, effect on the stacking fault energy (Ref 18). Manganese greatest effect is as an austenitizing element, and is essentially a replacement for some of the nickel in these alloys, making them more economical.

In a previous study (Ref 4), 21-6-9 was shown to have excellent ductility, with elongations to failure between 55 and 95%. Data showed a decrease in ductility from room temperature to 700 °C, followed by an increase in ductility to 1200 °C. Essentially, there appears to be a minimum in the materials ductility at roughly 700 °C.

Figure 6 shows the effect of grain size on the strength,

$$\sigma_y = \sigma_0 + k_y \left(\frac{d}{b}\right)^{-1/2} \quad \text{(Eq 4)}$$

(σ_y is the yield strength, k is a constant, and d is the average grain diameter). In the present case, the term σ_0 represents the intrinsic strength of the material (i.e., the strength of a solution annealed single crystal). The constant k is assumed independent of the narrow range of strain rates. Figure 6 is a graph of yield strength versus the reciprocal square root of the average boundary intercept, $d^{-1/2}$. Data are plotted for two strain rates along with data from a similar study (Ref 4). The best fit value for k is 503 MPa $\cdot \mu m^{-1/2}$, σ_0 as 282 MPa for $\dot{\varepsilon} = 10^{-3}\ s^{-1}$ and $T = 20$ °C. As expected, 21-6-9 exhibits standard grain size strengthening similar to other austenitic stainless steels.

4. Conclusions

(1) The yield strength and strain-rate sensitivity, m, of solution annealed 21-6-9 austenitic stainless steel was determined over a wide range of

   a. Temperature (−196 to 1100 °C)
   b. Strain rate (10^{-4} to 10^{4} s^{-1})
   c. Grain-size (26 to 104 μm).

(2) m dramatically increases above 850 °C from about 0.02 to 0.20.
(3) The mechanism of plastic flow is constant from ambient temperature to 750 °C over 10^{-4} to 10^{4} s^{-1} strain rate. This is consistent with transmission electron microscopy observations.
(4) Grain-size strengthening is observed.

References

1. D.J. Alexander and G.M. Goodwin, Thick-Section Weldments in 21-6-9 and 316LN Stainless Steel for Fusion Energy Applications, *J. Nucl. Mater.*, 1992, **191-194**, p 691

2. R.R. Boyer, An Overview on the Use of Titanium in the Aerospace Industry, *Mater. Sci. Eng. A*, 1996, **213**, p 103
3. M.P. Oliver, The Results of Improper Manufacturing Techniques on 21-6-9 Stainless Steel Tubing, *Focus Mech. Fail. Mech. Detect.*, 1991, **9-11**, p 217
4. S.G. Torres and G.A. Henshall, Tensile properties of 21-6-9 stainless steel at elevated temperatures, Lawrence Livermore National Laboratory Report, UCRLID-114590, 1993
5. P. Landon, Lawrence Livermore National Labs, 1982, private communication
6. M.E. Kassner and R.D. Breithaupt, The Yield Stress of Type 21-6-9 Stainless Steel Over a Wide Range of Strain Rate (10-5-104s-1) and Temperature, *Mech. Prop. High Rates Strain*, 1984, **9-12**, p 47
7. G.A. Henshall and A.K. Miller, The Influence of Solutes on Flow-Stress Plateaus, with Emphasis on Back Stresses and the Development of Unified Constitutive-Equations, *Acta Metall.*, 1989, **37**(10), p 2693
8. C.G. Schmidt and A.K. Miller, The Effect of Solutes on the Strength and Strain-Hardening Behavior of Alloys, *Acta Metall.*, 1982, **30**(3), p 615
9. M.E. Kassner, *Fundamentals of Creep in Metals and Alloys*, 2nd ed., Elsevier, Amsterdam, 2009
10. M.E. Kassner, R.S. Rosen, and G.A. Henshall, Delayed Mechanical Failure of Silver-Interlayer Diffusion Bonds, *Metall. Mater. Trans. A*, 1990, **21**(12), p 3085
11. J.D. Campbell and W.G. Ferguson, Temperature and Strain-Rate Dependence of Shear Strength of Mild Steel, *Philos. Mag.*, 1970, **21**(169), p 63
12. T.L. Briggs and J.D. Campbell, Effect of Strain Rate and Temperature on Yield and Flow of Polycrystalline Niobium and Molybdenum, *Acta Metall.*, 1972, **20**(5), p 711
13. J. Harding, Effect of Temperature and Strain Rate on Strength and Ductility of 4 Alloy-Steels, *Met. Technol.*, 1977, **4**, p 6
14. R.E. Stoltz and J.B. Vandersande, The Effect of Nitrogen on Stacking-Fault Energy of Fe-Ni-Cr-Mn Steels, *Metall. Mater. Trans. A*, 1980, **11**(6), p 1033
15. C.L. Briant, Hydrogen Assisted Cracking of Type-304 Stainless-Steel, *Metall. Mater. Trans. A*, 1979, **10**(2), p 181
16. Z. Mei and J.W. Morris, Influence of Deformation-Induced Martensite on Fatigue Crack-Propagation in 304-Type Steels, *Metall. Mater. Trans. A*, 1990, **21**(12), p 3137
17. M. Nystrom, U. Lindstedt, B. Karlsson, and J.O. Nilsson, Influence of Nitrogen and Grain Size on Deformation Behaviour of Austenitic Stainless Steels, *Mater. Sci. Technol.*, 1997, **13**(7), p 560
18. D.T. Llewellyn, Work Hardening Effects in Austenitic Stainless Steels, *Mater. Sci. Technol.*, 1997, **13**(5), p 389